Anisotropic and Smooth Inductively Coupled Plasma (ICP) Etching of III-V Laser Waveguides using HBr-O_2 Chemistry

S. Bouchoule[a)], S. Azouigui, S. Guilet, G. Patriarche, L. Largeau, A. Martinez, L. Le Gratiet, A. Lemaitre

Laboratoire de Photonique et de Nanostructures (LPN), CNRS, Route de Nozay 91 460 Marcoussis, France

F. Lelarge

Alcatel – Thales III-V Lab, Route de Nozay 91 460 Marcoussis, France

****

The original version of this paper has been published by the Electrochemical Society (ECS) in the Journal of Electrochemical Society

J. Electrochem. Soc., vol. 155 (issue 10), pp. H778-H785, (2008)

DOI : 10.1149/1.2965790

****

Abstract :

HBr ICP etching is investigated to realize ridge laser waveguides on InP and GaAs substrates. It has been reported that pure HBr chemistry leads to undercut ridge profiles when a hard dielectric mask is used. In this paper we show that a passivation layer can build up on the sidewalls and prevent lateral etching at high ICP powers if a Si wafer is used as the sample tray. Ex-situ energy dispersive X-ray analysis coupled to transmission electron microscopy shows that the passivation layer is a Si-rich silicon oxide. Vertical sidewalls, very smooth etched surface, and moderate etch rate compatible with the processing of shallow ridge lasers, can be obtained for InP-based heterostructures. The optimized HBr etching process for is used to etch InAs Quantum Dot (QD) shallow ridge lasers grown on InP (100) substrate, and compared to a classical HCl selective chemical etch. The waveguide losses of the HBr etched waveguide do not differ from those of the chemically etched waveguide by more than 1 cm^{-1}. Finally, we show that a similar passivation mechanism can be obtained during HBr ICP etching of GaAs/AlGaAs ridge waveguides, demonstrating that the same HBr (-O_2) chemistry is suitable for both GaAs and InP systems.

[a)] Electronic mail : sophie.bouchoule@lpn.cnrs.fr

I. INTRODUCTION

The etching of ridge waveguides is an important building block for optoelectronic edge-emitting devices. In the case of InP-based devices, shallow ridge waveguides are generally fabricated using selective chemical etching of InP against InGaAsP etch-stop layers. However, a nearly vertical ridge profile is only obtained for a specific orientation of the waveguide relatively to the InP cristallographic planes on InP(100) substrates, i.e. for ridge waveguides aligned parallel to the (011) direction, and it cannot be obtained for heterostructures grown on other substrates orientation, such as InAs Quantum Dots (QDs) laser structures on $InP(311)_B$ substrate.[1] ICP etching represents a promising alternative, provided that smooth and vertical sidewalls, a smooth etched surface, and a moderate etch rate compatible with a reproducible etch stop on a thin quaternary layer can be obtained simultaneously.

Cl-containing gas mixtures are usually used for the ICP etching of III-V compounds. In this paper we explore using hydrogen bromide as an alternate halogen gas to etch laser heterostructures. Only few studies on high density plasma etching of InP have been devoted to date to HBr in contrast to chlorinated gas, despite early investigations on conventional capacitively-loaded reactive ion etching (RIE) showing that HBr could be a promising candidate for the processing of InP laser facets.[2] Br-containing mixtures have also been studied with other dry etching techniques such as ECR,[3] and CAIBE.[4] More recently, HBr ICP etching at near room temperature has been investigated in the context of the processing of microelectronic devices such as HEMT structures.[5] A smooth etched surface has been obtained in this temperature range, but the mesa profiles systematically showed a positive slope that should be related to the effect of the angle dependence on sputter yield, or to the presence of $InBr_x$ on the etched surface,[6] and that is unsuitable for ridge waveguide processing. HBr ICP etching at high temperature (> 150 °C) has been shown to lead to more anisotropic profiles[7,8] and to high InP etch rates (> 1.4 μm/min). However in both work by Y.-S. Lee et al.[7] and L. Deng et al.[8] it was reported that undercut profiles were systematically obtained when dielectric hard masks were used. Hard masks are however highly desirable since they provide a better selectivity against InP than resist, and are more easily processed with vertical sidewalls. It has been assumed in Ref. 7,8 that the undercut in InP was due to the highly chemical nature of the pure HBr process, and a passivating gas (N_2, CH_4) has been consequently added to obtain InP mesas with vertical sidewalls. More recently, anisotropic ICP etching of InP has also been reported with O_2 added to HBr.[9] However, the exact mechanism involved in the sidewall passivation leading to anisotropic etching has not been analyzed in any case to our knowledge.

In this paper we propose an optimized HBr ICP process adapted to the fabrication of InP-based ridge laser waveguides. Vertical ridge sidewalls, a very smooth etched surface, and a moderate etch rate compatible with a reproducible etch stop on a quaternary etch-stop layer can be obtained simultaneously. Using a 4-in. silicon wafer as the sample holder, we show that a highly anisotropic ridge profile can be obtained by increasing the ICP power. The surface smoothness and the etch rate can be controlled by adapting the pressure and the sample temperature. An etch rate of 800 nm/min is

obtained at a pressure of 1 mT, and it can be reduced to a moderate value of ~ 350 nm/min by reducing the pressure to ~ 0.30 mT. An rms surface roughness as low as ~ 0.40 nm is simultaneously obtained when the sample temperature is reduced to ~ 130 °C. EDX-TEM micro-analysis of the sidewall composition evidences that anisotropic etching is achieved thanks to a passivation mechanism involving mainly the redeposition of Si by-products on the ridge sidewalls. After a chemical restoration using a buffered HF and KOH chemical etching sequence, very smooth and highly vertical ridge sidewalls can be obtained. The complete process is successfully used to fabricate InAs/InP quantum dot shallow ridge lasers with low optical loss. Finally, we show that a similar passivation mechanism occurs during the etching of GaAs/AlGaAs waveguides heterostructures with a Si wafer used as the sample tray. We demonstrate that the deposition of the silicon oxide layer on the AlGaAs sidewalls can be significantly enhanced by adding a small amount of oxygen in the gas mixture. These results demonstrate that the same HBr (-O_2) chemistry is suitable for the anisotropic ICP etching of both InP- and GaAs-based waveguides and devices.

II. GENERAL ETCHING CONDITIONS

The structures used for the process optimization are bulk n-doped InP(100) and GaAs substrates. The wafers are patterned with a hybrid metal-dielectric hard mask defining 4-µm to 2-µm wide stripes and sub-µm diameter pillars, and consisting of 70-nm Cr deposited on a 600-nm PECVD SiN_x layer using the lift-off technique, with subsequent anisotropic etching of SiN_x by SF_6/CHF_3 RIE using Cr as a mask. The wafers are then cut into 7mm*7mm samples for the study. The samples are etched in a Sentech SI-500 planar triple antenna spiral antenna ICP etch system described in a previous work.[10] They are deposited on a 4-in holder (also named electrode coverplate or sample tray) that is mechanically clamped above the temperature-controlled RF-biased electrode, and is thermally coupled to it. A 4-in silicon wafer is used as a tray, following our previous observations that the reaction products of silicon with the halogen reactive gas (Cl_2, HBr ..) could have a strong influence on the plasma chemistry and on the InP etching process.[10] This configuration also corresponds to most commercial ICP etch systems having an electrode diameter of 4-in or more, and used to etch III-V samples with typical dimensions of 2-in or less. The samples are either sticked to the Si holder or left thermally decoupled (no heat conducting grease used to attach the samples to the holder). In the latter case, the sample should be considered as thermally isolated from the electrode, and its surface temperature mainly imposed by the plasma conditions. If not specified in the following etching experiments, the rf power applied to the electrode is adapted to maintain a fixed dc bias value of –140 V, corresponding to the typical dc bias value previously optimized for the etching of InP-based deep ridge hetrostructures using Cl_2-H_2 chemistry.[10] The pressure is kept to a low value in the typical range of 0.25 mT to 2 mT. This is of importance for the passivation effects that occur on the III-V etched sidewalls. First a reduction in the lateral etch rate of the III-V material can be expected due to the reduced concentration of reactive species. Second, separate measurements performed in our etch

system have shown that the plasma potential is increased when the pressure is decreased, from a typical value of 15 V in the 5 mT – 10 mT pressure range, to values of more than 30V below 0.5mT.[11] The ion flux measured at the reactor walls with a RF planar probe [12] is also found to first increase with pressure in the 0.15 mT – 1 mT range, and then to gradually decrease with pressure for pressure values above 1 mT, thus showing a maximum around 0,5 mT – 2 mT. Both effects contribute to an enhanced bombardment of all the reactor surfaces including the reactor walls and also the Al_2O_3 ceramic parts of the reactor (coupling window and clamping ring) at low pressure, which may in turn enhance the sputtering effect and chemical reactions at the surfaces, and the desorbed species have to be taken into account in the passivation effects.

Finally two kinds of laser epitaxial structures have been used for laser shallow ridge waveguide etching. The InP-based structures grown by MBE on a n-doped InP(100) substrate consists of an InP:n buffer layer, an InGaAsP (λ_g = 1.17μm) waveguide including 6 InAs QD planes, an InP:p spacing layer, a 35nm InGaAsP:p etch stop layer, a 1.7-μm thick InP:p layer, and an InGaAs:p^{++} contact layer. The GaAs-based structure grown on a n-doped GaAs substrate by MBE consists of a n-doped 1.5-μm thick Al_{80}GaAs bottom cladding layer, a 350-nm thick GaAs waveguide including a InGaAsN/GaAs quantum-well active layer, a p-doped 1.5-μm thick Al_{80}GaAs top cladding layer capped with a p^{++}-doped GaAs contact layer. As for the bulk samples, a SiN_x/Cr mask is used to define the waveguide stripes.

III. HBr ICP ETCHING OF InP

A. INFLUENCE OF ICP POWER

Figure 1 shows the InP etch rate measured for HBr plasma at 1 mT pressure and –140V dc bias as a function of ICP power for both thermalized and non-thermalized samples. The positive ion current density measured at the reactor walls with the RF planar probe is also reported in the figure. Below a typical ICP power value of 150 W, the etch rate is low, and the etched surface of non-thermalized samples is rough indicating that the flux of ions impinging the surface is not sufficient to elevate the sample at the necessary temperature. This is consistent with the ion current density curve, showing that the on-set of the high density inductive mode occurs at an ICP power above ~150 W in our system. Separate measurements of the InP etch rate performed with thermalized samples showed that an electrode temperature higher than 140 °C is required to obtain a smooth etched surface at a pressure of 1 mT. The ion current density continuously increases with the ICP power in the 50 W - 1100 W range, but the InP etch rate tends to saturate to a typical value of 800 nm/min at high ICP powers for thermalized samples, and even shows a decrease for the non-thermalized samples at high ICP power after a maximum value of ~ 950 nm/min has been achieved around 400 W ICP power. This etch rate behaviour is roughly independent of the electrode temperature for non-thermalized samples (thermally decoupled from the electrode), as illustrated in Figure 2 for an electrode temperature of 100 °C. The etch rate of the 4-in Si coverplate rate has been simultaneously measured by patterning the Si wafers

with a dielectric mask forming 20-µm wide ridge mesa spaced by 500 µm in the centre area of the wafer, and typical results are also reported in Fig. 2. It has been observed that the 4-in Si wafer etch rate is only weakly dependent on the cathode temperature in the 100 °C – 190 °C temperature range (less than 20 % decrease in the etch rate is observed when the cathode temperature is increased from 100 °C to 190 °C for fixed plasma parameters), and in any case a saturation of the Si etch rate appears as for the InP etch rate, despite the increase in positive ion current density. This has to be related to a reactant-limited etching regime at high ICP powers. Optical emission spectroscopy and actinometry measurements performed in the HBr plasma as a function of ICP power have indeed revealed that the concentration of the Br radical saturates at high ICP powers.[13]

The main interesting result obtained at high ICP power concerns the ridge profile, as shown in Figure 3 for the non-thermalized samples. While a strongly undercut profile resembling that reported in Ref. 7 is observed at moderate ICP powers (200 W - 700 W), a transition to an almost vertical profile occurs when the ICP power is further increased. The etching profile of Fig. 3(d) indicates that a passivation layer is redeposited on the etched sidewalls. We recently conducted a systematic study of the passivation layer deposited on the sidewalls of InP sub-micron diameter pillars etched in Cl_2-H_2/N_2 and HBr inductively coupled plasmas using TEM-EDX ex-situ analysis.[14] Briefly, the procedure consists in dispersing the etched micropillars cut from the substrate on a carbon membrane for TEM inspection of the pillars sidewalls. The presence of any passivation layer different from InP can be detected with a spatial resolution better than 1 nm, and the composition of this layer can be estimated with a typical spatial resolution of ~ 5 nm using the EDX spectroscopy system installed in the microscope with the transmitted electron beam as the excitation source. Since the passivation layer deposited on the sidewall of ridge patterns should be very similar to that deposited on pillars sidewalls, the same procedure has been applied for HBr with the above plasma parameters (1000W ICP power, -140 V dc bias, 1 mT) and the obtained results are reported in Table I (case A). A TEM image of the sidewall of one of the micropillars deposited on the TEM carbon membrane is shown in Figure 4. The etch depth was fixed to ~ 2 µm. It is observed that a Si-rich silicon oxide passivation layer resulting from the etching of the 4-in Si-wafer is deposited on the InP sidewall at high ICP powers, that acts as an etch inhibitor to prevent lateral etching and undercut of the InP ridge patterns. The 4-in Si wafer etch rate measured under the same etching conditions has been found to be of ~ 140 nm/min (see Fig. 2) which corresponds to an equivalent Si flux of ~ 1.8 sccm if one considers a Si density of 5 10^{22} at/cm^3. Although defining an equivalent Si flux is only a very qualitative approach since it does not differentiate the different by-products that are produced in the gas phase due to Si etching, this figure indicates that a small quantity of Si-based precursors is sufficient to form a passivation layer inhibiting lateral etching. In our experiments the size of the InP sample is small, and it may be expected that the passivation mechanism will be reduced or even suppressed if the InP sample size is increased and the uncovered surface of the Si wafer is decreased. We have therefore compared the etching results obtained for a 7 mm*7 mm sample and for a 2-in InP wafer patterned with ~ 2-µm wide ridge stripes.

The InP etch rate measured for the 2-in wafer is reduced by ~ 50 % compared to the case of small InP sample due to loading effects, but an etching profile identical to that presented in Fig. 3-(d) has been observed in both cases. This result indicates that even a smaller concentration of Si-by products in the gas phase may be sufficient to allow for the passivation layer to build-up. However, in the limit case where the diameter of the InP wafer to be etched will completely cover or even replace the Si tray, it can be predicted that the anisotropic etching will not be maintained if the gas mixture is not changed. A similar effect can also be anticipated if the Si wafer carrier surface is covered by a material (resist, polymer, dielectric,..) that is only slowly etched or that does not contains silicon.

Finally, it is observed from Fig. 3 that an anisotropic etching profile is obtained at high ICP power (above 800 W), while undercut profiles are observed at low ICP powers (< 200 W) for which the Si etch rate is low, but also at moderate ICP powers (around 300 W – 600 W) for which the 4-in Si etch rate is very similar to that measured at higher ICP powers as reported in Fig. 2. Diagnostics of the gas phase such as optical spectroscopy or mass spectroscopy are necessary in order to precisely explain this behavior, however we believe that two effects may explain the underetching observed when the ICP power is reduced. First it is observed from Fig. 2 that the InP etch rate saturates at high ICP powers despite the fact that the positive ion density continuously increases. This may indicate that the etching is limited by the reactive radicals available at the surface, and it can be expected that the lateral etch rate of the sidewall will also saturate. Second, the results of Table I reveal that the passivation layer contains a significant amount of oxygen. Oxygen incorporation may result from the exposure at ambient air since the TEM-EDX analysis is performed ex-situ, but we believe that a minimum amount of oxygen is required in the plasma to allow for the passivation layer to build-up, even in the case of a Si-rich (Si/O > 1) passivation layer. In-situ or quasi-in-situ sidewall characterization methods have to be developed to confirm this assumption, which is presently not feasible in our reactor system. Nevertheless our hypothesis is consistent with extensive studies performed in the context of sub-100nm Si-gate etching in HBr-Cl_2-O_2 inductively coupled plasma, [15] showing that anisotropic Si-gate etching is obtained thanks to the deposition of a SiOCl(Br) layer on the gate sidewall, and that oxygen needs to be present in the gas phase. Although oxygen is not intentionally added in our case, the possible sputtering or the desorption of oxygen from the inner parts of the reactor (Al_2O_3 parts, but also reactor walls that are conditioned by the preceding etching steps) will be maximum at high ICP powers due to the higher positive ion flux, and the passivation mechanism can be favoured. The conjunction of a reactant-limited etching regime, and the possible increase in the concentration of the precursors of the passivation layer in the gas phase, may thus account for the onset of the anisotropic regime. On the contrary, it can be speculated that lateral etching may enter in competition with sidewall passivation when the ICP power is reduced due to a higher radical concentration near the surface and/or a lower concentration of the passivation layer precursors in the gas phase, and that the net result will be the apparition of underetching.

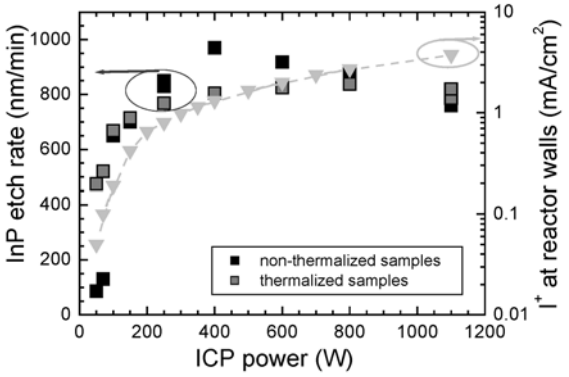

Figure 1: InP etch rate (left axis) of thermalized (grey squares) and non-thermalized samples (black squares), and positive ion current density (right axis, light grey triangles) measured as a function of ICP power. The dashed grey line is a guide to the eyes for the positive ion current density. Other etching parameters are 1 mT pressure,–140 V dc bias, 10 sccm HBr flow-rate, and electrode temperature fixed to 190 °C.

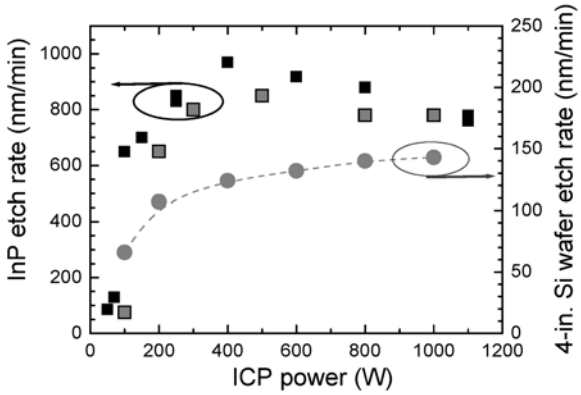

Figure 2: InP etch rate (left axis, grey squares) of non-thermalized samples measured as a function of ICP power for an electrode temperature of 100 °C. The etch rate obtained for an electrode temperature of 190°C is also reported for comparison (left axis, black squares). The 4-in Si wafer etch rate (right axis, grey circles) measured as a function of ICP power is reported for an intermediate temperature of 150 °C. The other etching parameters are identical to Fig. 1.

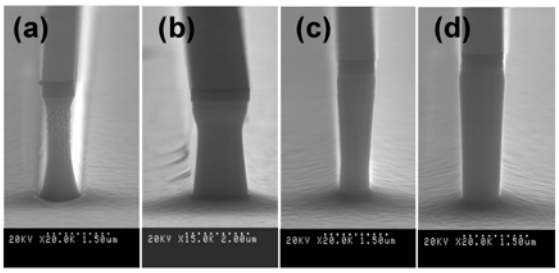

Figure 3 : SEM images of the ridges profiles etched with an ICP power of 200 W (a), 500 W (b), 800 W (c), and 1000 W (d) in the case of non-thermalized samples. The other etching conditions are those of Fig. 1.

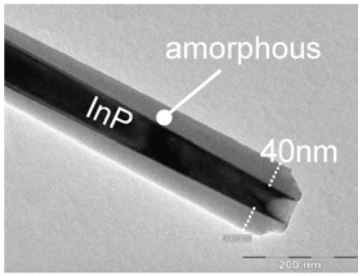

Figure 4: Typical TEM image of the top an InP sub-µm micropillar etched with the HBr chemistry. The amorphous layer is apparent on the sidewalls.

Table I: InP or GaAs etch rate, 4-in Si wafer etch rate, average thickness of the passivation layer measured on the top part of the pillar by TEM, and average passivation layer composition in atomic percentage deduced from EDX analysis. In the case (B) for GaAs etched with pure HBr, the thickness of the passivation layer is smaller than the ~ 5 nm spatial resolution of the EDX-analysis.

Process		Etch rate, nm/min			Passivation layer							
Ref	Material / Etching gas	InP	GaAs	4-in Si	Thickness (nm)	Average composition (atomic %)						
						Si	O	Br	Cl	P	In	Al
A	InP / HBr (1000 W)	830	--	140	40	65	20	9	--	6	--	--
B	GaAs / HBr	--	600	155	4	38	62	--	--	--	--	--
C	GaAs / HBr-O_2	--	670	176	30	35	63	2	2	--	--	--

B. INFLUENCE OF PRESSURE AND TEMPERATURE

Despite the fact that the vertical sidewall profile obtained in the above experiments may be suitable for the definition of ridge waveguides, the etch rate is still high, and a reproducible and precise control of the etching depth, as required for the fabrication of shallow ridge waveguide lasers, is difficult. Reducing the working pressure is an efficient way to reduce the etch rate as reported in Figure 5-(a). The HBr flow-rate was adapted for each pressure value in order to maintain the ~ same pumping speed and the same gas residence time in all cases. It is close to the maximum value allowed by our pumping system, and is of 27 sccm for 1 mT pressure. A moderate InP etch rate of ~ 350 nm/min with a vertical sidewall profile is obtained at a working pressure of ~ 0.30 mT. The 4-in Si wafer etch rate measured in the same plasma conditions is reported in Figure 5-(b). The measured etch rates correspond to an equivalent Si flux in the plasma of 0.9 sccm, 1.3 sccm and 1.8 sccm, for 0.30 mT, 0.50 mT and 1 mT, respectively. Figure 6 shows that an anisotropic ridge profile is maintained until the low pressure value of ~ 0.25 mT thanks to the same Si-based passivation mechanism. Reducing further the pressure induces a change in the etching regime, and a positively sloped profile with significant micro-trenching at the bottom of the ridge is obtained for low pressure values below 0.15 mT, which may be due to too strong passivation effect. At low pressure the concentrations of radicals involved in the chemical etching is also reduced, while the positive ion flux is still high (a positive ion current density higher than 1.4 mA/cm^2 is measured at the reactor walls with the rf planar probe, as reported in Fig. 5-(b)), which may favor the physical component of the etching.

We have previously evidenced that the sidewalls of InP patterns etched with the HBr chemistry can be very smooth.[14] The sidewall roughness can be of critical importance for photonic elements such as deep ridge waveguides, deeply etched vertical Bragg mirrors or facets. In the case of shallow ridge waveguides, the roughness of the etched surface can be more detrimental to the optical loss of the guided mode, since the optical mode extends laterally close to the InP / air interface. Unfortunately, it can be observed from the SEM images that the InP etched surface of non-thermalized samples is somewhat rough. The exact mechanism responsible for the observed surface roughness needs further investigation, however, it can be expected in our case that the InP surface is elevated at a very high temperature (> 190°C) at high ICP powers when the samples are non-thermalized, due to the high ion flux. An unbalanced etching of In and P elements, or a competition between InP etching and Si by-products adsorption on the InP surface, at very high temperature, might be considered as possible mechanisms to investigate the apparition of roughness. The surface roughness is significantly reduced when the samples are thermalized as can be deduced from Figure 7 comparing the etched surface of a thermalized and non-thermalized InP sample etched at a pressure of 1 mT, ICP power of 800 W, and dc bias of −140 V. The cathode temperature is fixed to 190 °C in this experiment to favor the desorption of $InCl_x$ products. Fig. 7 also evidences that a lateral undercut is systematically observed for the thermalized sample. Decreasing the pressure down to 0.3 mT allows for obtaining simultaneously a vertical sidewall and a low etched surface roughness when the samples are

thermalized as illustrated by the SEM images of Figure 8. Moreover, at such a low pressure, the electrode temperature can be reduced from 190 °C down to 130 °C without changing the etching results. This is an advantage of the low-pressure value: a significant roughness related to the low volatility of $InCl_x$ products appears at an electrode temperature of 130°C as soon as the pressure is higher than 0.5 mT. AFM measurements have been carried out to quantitatively compare the surface roughness of non-thermalized and thermalized etched samples etched at a pressure of 0.30 mT and 1 mT. The obtained results are listed in Table II. A very smooth surface showing a rms roughness (3x3 μm^2 measurement window) as low as 0.43 nm is obtained for thermalized samples etched at a pressure of 0.3 mT with an electrode temperature fixed to 130 °C. Finally it has been observed that at 0.30 mT pressure the Si-based passivation mechanism is sufficient to guarantee an anisotropic ridge profile for ICP power values in the range from 1100 W to ~ 600 W. The surface roughness is kept unchanged and low in this power range. Reducing further the ICP power leads to the onset of sidewall undercutting.
Following this process optimization, the etching parameters have been fixed to the following values for the next experiments: ICP power of 800W, dc bias of -140 V, pressure of 0.3 mT, HBr flow-rate of 8 sccm, electrode temperature of 130 °C, thermalized samples.

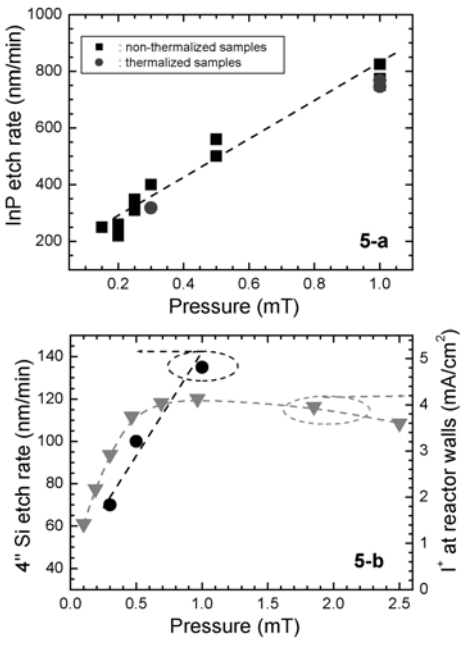

Figure 5 : (a): Etch rate of non-thermalized InP samples (squares) measured as a function of pressure. The etch rate of thermalized InP samples (circles) measured at a pressure of 1mT and 0.30mT is also reported. The other etching parameters are 1000 W ICP power, –140 V dc bias, electrode temperature fixed to 150 °C. The HBr flow-rate is adjusted for each pressure value to maintain a ~ constant gas residence time (27 sccm at 1 mT and 4 sccm at 0.15 mT). (b): 4-in Si wafer etch rate (left axis, circles), and positive ion current density (right axis, triangles) measured as a function of pressure under the same etching conditions. Dashed lines are guide to the eyes.

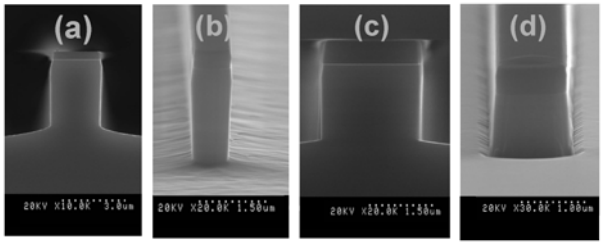

Figure 6 : SEM images of the ridges profiles etched at a pressure of 1 mT (a), 0.5 mT (b), 0.30 mT (c), and 0.10 mT (d) in the case of non-thermalized samples. The other etching conditions are 1000 W ICP power, -140 V dc bias, cathode temperature fixed to 150°C. The HBr flow rate is adapted for each pressure value to maintain a ~ constant gas residence time (27 sccm for 1 mT and 2.7 sccm at 0.10 mT)

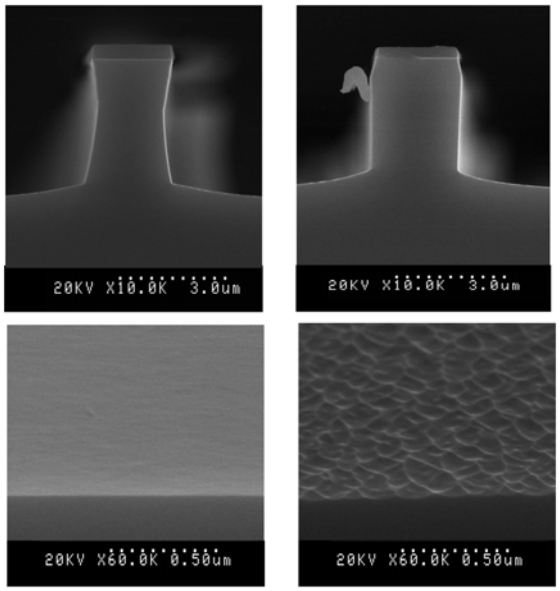

Figure 7 : Top : SEM images of the ridge profile for a thermalized sample (left) and a non-thermalized sample (right) simultaneously etched at a pressure of 1 mT. Bottom : Roughness of the etched InP surface observed at 2° off from normal incidence for the thermalized (left) and the non-thermalized (right) samples. The other etching conditions are 1000 W ICP power, -140 V dc bias, 27 sccm HBr flow-rate, and cathode temperature fixed to 190 °C.

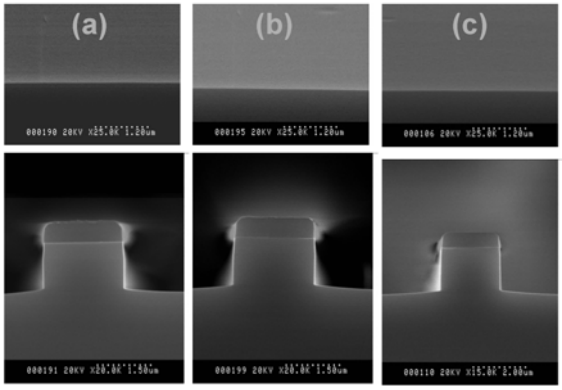

Figure 8 : SEM images of the ridge profile (bottom) and roughness of the etched surface observed at 2° off from normal incidence for thermalized InP samples etched with an electrode temperature of 130 °C (a), 150 °C (b), and 190°C (c). The other etching conditions are 800 W ICP power, -140 V dc bias, 0.30 mT pressure, 8 sccm HBr flow-rate.

Table II :AFM measurements of the rms and peak-to-valley surface roughness of InP samples etched with HBr chemistry for a non-thermalized and a thermalized sample etched simultaneously at a pressure of 1 mT and an electrode temperature of 150°C (I), and for thermalized samples etched at 0.30 mT and an electrode temperature of 190°C (II), 150 °C (III) and 130 °C (IV). The other etching parameters are 1000 W ICP power and –140 V dc bias. The HBr flowrate is fixed to the highest flow-rate at a given pressure. The measurement window is of 3x3 μm^2. The surface roughness of an un-etched sample is given as a reference.

Process				**Surface roughness (AFM)**	
Run #	Pressure (mT)	Temperature (°C)	Sample thermalization	rms (nm)	peak-to-valley (nm)
I	1	150	nonthermalized	2.60	35.9
I	1	150	thermalized	0.48	12.5
II	0.30	190	thermalized	0.45	6.2
III	0.30	150	thermalized	0.50	6.9
IV	0.30	130	thermalized	0.43	6.4
--	*un-etched reference sample*			0.21	3.8

C. POST-ETCH RESTORATION OF THE SIDEWALL SURFACE

It has been shown in section A consistently with our previous work[14], that the passivation layer deposited on the InP sidewalls during HBr ICP etching is a Si-rich silicon oxide, with an ex-situ Si composition in atomic percentage around 65 %. Such a material can easily be selectively removed from the InP surface using silicon oxide or silicon chemical etchants. A Si chemical etchant that does not etch the SiN_x mask may be preferred if the mask has to be preserved for subsequent fabrication steps. This can be for instance required for the fabrication of buried ridge stripe lasers relying on a selective lateral epitaxial regrowth. A diluted KOH solution can be used to remove the Si-rich layer from the InP sidewalls for this purpose. Figure 9 compare the SEM images of the ridge profile of InP samples etched for 5 min just after the etching step (Fig. 9-(a)), and after a chemical post-etch restoration of the sidewall (Fig. 9-(b,c)). In the latter case the sample was first dipped for 10 s in an amonium fluoride (AF) mixture to remove any native oxide that readily forms on the Si-rich passivation layer under air exposure, and then etched for 1 min in a 40% vol. KOH solution at a temperature of ~ 30°C. SEM inspection clearly shows that the ridge sidewall has been modified by the post-etch restoration, as reported in Fig. 9: it appears to be more vertical and smooth. Although EDX-TEM analysis of the sidewall of InP micropillars has not been carried out after the post-etch restoration step in order to definitely prove this assumption, it is considered that the change in the ridge profile indicates that the KOH solution can successfully remove the Si-rich passivation layer. Fig. 9-(b) also indicates that the roughness of the etched surface has not been modified by the post-etch restoration.

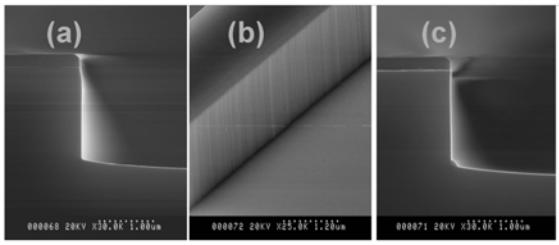

Figure 9 : SEM images of the ridge profile of an InP sample etched with the optimized conditions after the etching step (a), and after the chemical post-etch step (b), (c).

IV. InAs/InP QD SHALLOW RIDGE WAVEGUIDE PROCESSING

In order to qualify the HBr process, InAs/InP QD 2-µm wide (single transverse mode) shallow ridge waveguide lasers have been processed from the vertical structure described in section II, and their performances have been compared to that of shallow ridge lasers chemically etched using a classical selective HCl/H_3PO_4 solution. In the case of the dry etched waveguides, the etch depth is monitored using an in-situ laser reflectometry system and the etching is stopped at a distance of ~ 40 nm (corresponding to a half-period on the reflectometry curve) above the 30-nm thick quaternary etch-stop layer. The Si-rich passivation layer is then removed from the ridge sidewalls using the AF / KOH

etching sequence. Eliminating the silicon oxide layer from the ridge sidewall is not critical in the case of shallow ridge waveguides, since the optical modal losses will rather originate from the surface roughness than from the presence of a lossy layer on the ridge sidewall. The post-etch restoration step is however performed in order to eliminate this possible issue. In the case of the chemically etched lasers, only the 200-nm thick InGaAs:p^{++} top layer is dry-etched, while the InP cladding layer is selectively wet-etched down to the InGaAsP etch-stop layer. A thin PECVD SiN_x layer is then deposited on the samples, followed by a benzocyclobutene (BCB) planarization step. A contact window is opened on the top of the ridge (SF_6/O_2 RIE) and a Ti-Au electrical contact layer is evaporated. After substrate thinning and evaporation of the n-type backside contact, laser arrays of several lengths are cleaved for optical characterization.

The threshold current density measured as a function of the inverse of the laser length is reported in logarithmic scale in Fig. 10-(a) for the dry-etched and the wet-etched lasers. Very similar threshold currents are obtained for both laser types. A threshold current density at infinite length corresponding of ~ 310 A/cm^2 per QD plane can be deduced from the curve, very close to the value obtained from broad area laser processing with the same structure. The inverse of the laser external efficiency measured as a function of laser length is reported in Fig. 10-(b). The moderate value of the internal quantum efficiency (~40%) is very similar to that obtained from broad area laser processing and is thus linked to the epitaxial structure used here to compare the dry and chemical etching approaches, having a low confinement potential of the carriers in the quantum dots. The waveguide optical losses deduced from the slope of the external efficiency curves are of 8.5 cm^{-1}, and of 9.2 cm^{-1} for the dry-etched lasers and the chemically etched lasers, respectively. These values are different by less than 1 cm^{-1}, demonstrating the suitability of the HBr ICP etching process for shallow ridge waveguide laser fabrication.

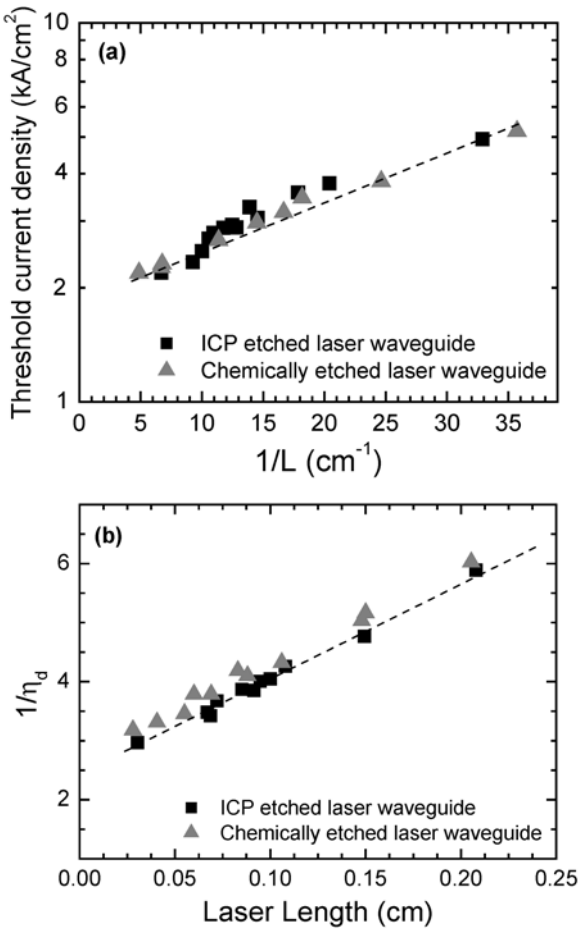

Figure 10: Laser threshold current density measured as a function of the inverse of the laser length (a), and inverse of the laser external quantum efficiency measured as a function of laser length (b) for the chemically etched (grey triangles) and the ICP etched (black squares) QD lasers with 6 QD planes.

V. COMPARISON TO GaAs HBr ICP ETCHING

Anisotropic etching of GaAs based-structures has already been reported in HBr-containing inductively coupled plasmas. An additive gas considered as a passivating gas, such as N_2, has been added to HBr in order to obtain highly vertical profiles.[5] It is worthwhile to investigate if anisotropic etching of GaAs-based laser waveguides can be obtained in our case using HBr as the reactive gas when a 4-in Si wafer is used as the sample tray, and if the anisotropy is related to the same Si-based passivation mechanism as for InP. Bulk GaAs:n samples have been used for this purpose.

A typical GaAs ridge profile etched with HBr is reported in Figure 11-(a). The etching parameters are 1000 W ICP power, –160 V dc bias, 1 mT pressure, an HBr flow-rate of 27 sccm, an electrode temperature of 30 °C, thermalized sample. The GaAs etch rate is of 600 nm/min. The 4-in Si wafer etch rate simultaneously measured is found to be of 155 nm/min. A fully passivated GaAs sidewall is not obtained: the bottom part of the ridge is slightly positively sloped, while the upper part exposed a longer time to the plasma is negatively sloped indicating that some undercutting still occurs. A more pronounced undercut profile (and a higher etch rate) is obtained for a non-thermalized GaAs sample. Sub-micron GaAs pillars were etched to an etch depth of ~2 µm using the same etching process for TEM-EDX analysis of the sidewall composition. The results are reported in Table I (case B). A Si-rich

passivation layer exists but its thickness is significantly reduced compared to the case of InP. The same observation could be done for a non-thermalized sample. This indicates that a passivation mechanism involving the Si by-products may also take place during the etching of GaAs-based samples, but that the effective passivation layer deposition rate is lower on the GaAs surface that on the InP surface. The composition of the passivation layer is also found to be very close to SiO_2 instead of being Si-rich as previously found on the sidewalls of InP patterns. However this may not correspond to an actual difference in the in-situ composition of the passivation layers, due to the very low thickness of the layer for the GaAs case. It has indeed already been reported in the context of Si gate etching using $Cl_2/HBr/O_2$ inductively coupled plasmas that Cl or Br desorption and exchange with O take place when a Si surface covered by a SiOCl or SiOBr passivation layer is brought back to ambient air after etching.[15] For this reason, when the passivation layer thickness is less than few nanometers, it becomes difficult to extrapolate the in-situ composition of the passivation layer that builds-up during etching on the III-V sidewall, from ex-situ measurements.

It has already been shown that adding O_2 to a chlorine-based plasma also containing silicon can favour the passivation of the GaAs sidewall thanks to the deposition of a SiO_2-like passivation layer. O_2 has for instance been added to a $SiCl_4/N_2$ inductively coupled plasma to obtain anisotropic etching of GaAs/AlGaAs periodic structures.[16] In our case where HBr is used as a reactive gas and where Si by-products exist in the plasma due to the etching of the 4-in silicon coverplate, the passivation mechanism could thus be enhanced by adding a small amount of oxygen. Figure 11-(b) shows the ridge profile obtained under etching conditions similar to that of Fig. 11-(a), with 5 % of O_2 added to the gas mixture. It can be observed that the GaAs sidewall is fully passivated and highly vertical. TEM-EDX analysis of the sidewall composition has been carried out from sub-micron GaAs pillars etched to an etch depth of ~ 2 μm using the same etching process, and the results are reported in Table I (case C). The passivation layer is significantly thicker in case C, than in case B without intentional O_2 addition, and its composition is very close to SiO_2. Another effect of O_2 addition to HBr is to increase the etch rates of both the GaAs and Si materials: they are measured to be of 670 nm/min and 176 nm/min for GaAs and Si, respectively for 5% of O_2 added to the gas mixture. Early spectroscopic studies on Cl_2/O_2 plasma have shown that the dissociation of chlorine is enhanced when a small amount of O_2 is added to the gas mixture,[17] and the latter observation indicate that a similar effect may occur with HBr.

Finally it is found that the GaAs etch rate is generally smaller than the InP etch rate: for 1000 W ICP power, 1 mT pressure, and -140 V dc bias it is measured to be of 530 nm/min and 850 nm/min for GaAs (thermalized sample) and InP (non-thermalized sample), respectively. The silicon oxide passivation mechanism of the GaAs sidewalls is maintained when the pressure is reduced down to 0.5 mT, however, the GaAs etch rate is further reduced at the same time, and reducing further the pressure leads to selectivity issues against dielectric mask. For this reason, the ICP power and pressure values have been kept at 1000 W and 1 mT for the etching of the GaAs material.

The HBr-O_2 process has been used for the etching of a shallow ridge laser waveguide from the AlGaAs/GaAs waveguide epitaxial structure described in section II. An SEM image of the shallow waveguide cross-section is reported in Figure 12. Passivated, smooth, and vertical sidewalls together with a smooth etched surface are obtained, demonstrating that the passivation mechanism based on Si by-products is also of great interest to obtain anisotropic profiles during HBr ICP etching of GaAs/AlGaAs structures.

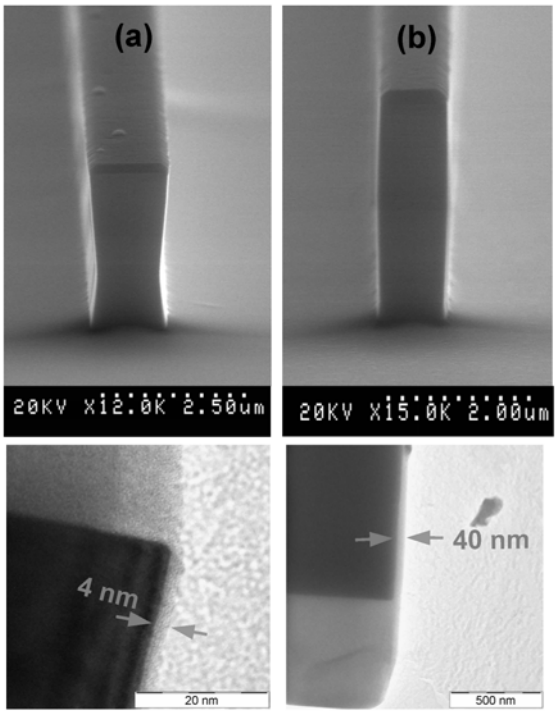

Figure 11: Typical SEM images of the GaAs ridge profile (top) and TEM images of sub-µm pillar sidewall used for EDX-TEM analysis of sidewall composition (bottom), etched using HBr chemistry (a), and HBr-O_2 chemistry with 5% of O_2 (b). The other etching parameters are 1 mT pressure, -140 V dc bias, 1000 W ICP power, 27 sccm total flow-rate, electrode temperature of 30 °C, sample thermalized.

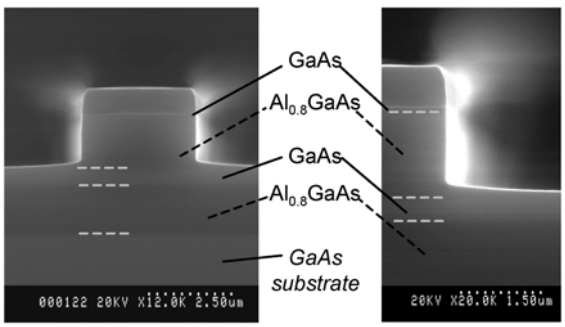

Figure 12: Typical AlGaAs/GaAs ridge profile obtained after etching using the HBr-O_2 chemistry with 5 % of O_2. The other etching parameters are those of Fig. 12.

VI. CONCLUSION

We have shown that smooth and anisotropic ICP etching of both InP and GaAs waveguides can be obtained using HBr chemistry. We have identified that in both cases, the same passivation mechanism based on the deposition of a silicon oxide layer on the etched sidewall allows for obtaining the etching anisotropy when a Si wafer is used as the sample tray. Only a small amount of Si (typical equivalent flow-rate of 1 scm or less) is sufficient to achieve the passivation effect. Moreover, consistently with earlier studies on Si gate etching with HBr-Cl_2-O_2 inductively coupled plasma we consider that a small

amount of oxygen is required to allows for the passivation layer to build up. In the case of HBr etching without O_2 intentional addition, we suggest that oxygen comes from the sputtering of the inner parts of the reactor at high ICP powers and high positive ions current, particularly at low pressure when the plasma potential is increased. Vertical, very smooth etching of InP –based waveguides together with a moderate etch rate compatible with a precise control of the etch stop can be obtained under these conditions, and QD lasers with low internal cavity loss have been successfully fabricated. Moreover, we have shown that anisotropic etching of GaAs and of AlGaAs/GaAs waveguides is also possible using the same passivation mechanism. Adding a small amount (< 5%) of oxygen to the gas mixture can strongly enhance the passivation effect in this latter case. Our results demonstrate the potential of the HBr – O_2 chemistry to etch III-V material photonic devices, when silicon is also present in the plasma phase. For completeness, in future industrial conditions where the diameter of the InP or GaAs wafer to be etched may be larger than 2-in and may completely cover or even replace the Si tray, it can be predicted that the anisotropic etching will not be maintained if the gas mixture is not changed. From our results, we propose that the addition of a small amount of a Si-containing gas to the HBr (-O_2) mixture could allow for maintaining anisotropic etching with a similar sidewall passivation mechanism.

ACKNOWLEDGEMENTS

The authors thank C. David of LPN for his support in AFM measurements. Dr. P. Chabert from Laboratoire de Physique et Technologie des Plasmas (LPTP), CNRS – Ecole Polytechnique, France, is gratefully acknowledged for providing the rf planar probe, and for fruitful discussions on plasma-surface interactions.

References

[1] G. Moreau, K. Merghem, A. Martinez, S. Bouchoule and A. Ramdane, F. Grillot, R. Piron, O. Dehease, E. Homeyer, K. Tavernier and S. Loualiche, P. Berdaguer, and F. Pommerau, EIT Optoelectronics, **1,** 255 (2007).

[2] K. Takimoto, K. Ohnaka, and J. Shibata, Appl. Phys. Lett, 50, 1947 (1989).

[3] S. J. Pearton, U. K. Chakrabarti, E. Lane, A. P. Perley, C. R. Abernathy, and W. S. Hobson, J. Electrochem. Soc.,139, 856 (1992)

[4] J. M. Rossler, Y. Royter, D. E. Mull, W. D. Goodhue, C. G. Fonstad, J. Vac. Sci. Tecnol. B, 16, 1012 (1998)

[5] D. Lishan, J. Lee, and G. Kim, GaAs MANTECH, Las Vegas, 2001.

[6] S. Vicknesh, and A. Ramam, J. Electrochem. Soc., 151, C772 (2004)

[7] Y. S. Lee, M. DeVre, D. Lishan, and R. Weestreman, G. Kim, Postdeadline paper TuA2.6, 15th IPRM Conf., Santa Barbara, CA, USA, May 12-16, 2003.

[8] L. Deng, A. L. Goodyear, M. Dineen, Proc. SPIE, vol.5280, p.838, 2004.

[9] E.L. Lim, J.H. Teng, L.F. Chong, N. Sutano, S.J. Chua, S. Yeoh, J. Electrochem. Soc., 155, D47 (2008).

[10] S. Guilet, S. Bouchoule, C. Jany, C. S. Corr, and P. Chabert, J. Vac. Sci Technol. B, 24, 2381 (2006)

[11] C. S. Corr, S. Guilet, S. Bouchoule, and P. Chabert, unpublished.

[12] N. St. J. Braithwaite, J. P. Booth, G. Cunge, Plasma Sources Sci. Technol., **5**, 677 (1996)

[13] L. Gatilova, S. Bouchoule, S. Guilet, G. Patriarche, and P. Chabert, J. Vac. Sci. Technol. A (submitted).

[14] S. Bouchoule, G. Patriarche, S. Guilet, L. Gatilova, L. Largeau, and P. Chabert, J. Vac. Sci. Technol. B, 26, 666 (2008).

[15] L. Desvoivres, L. Vallier, and O. Joubert, J. Vac. Sci. Technol. B 19, 420 (2001).

[16] S. Golka, S. Schartner, W. Schrenk, and G. Strasser, J. Vac. Sci. Technol. B **25**, 837 (2007).

[17] S. K. Murad, N. I. Cameron, S. P. Beaumont, and C. D. W. Wilkinson, J. Vac. Sci. Technol. B **14**, 3668 (1996).